Journal of Colloid and Interface Science 448 (2015) 275–279

Contents lists available at ScienceDirect

Journal of Colloid and Interface Science

www.elsevier.com/locate/jcis

Microfluidic generation of uniform water droplets using gas as the continuous phase

Kunqiang Jiang [a], Annie Xi Lu [b], Panagiotis Dimitrakopoulos [b], Don L. DeVoe [c,*], Srinivasa R. Raghavan [a,b,*]

[a] Department of Chemistry and Biochemistry, University of Maryland, College Park, MD 20742, United States
[b] Department of Chemical and Biomolecular Engineering, University of Maryland, College Park, MD 20742, United States
[c] Department of Mechanical Engineering, University of Maryland, College Park, MD 20742, United States

GRAPHICAL ABSTRACT

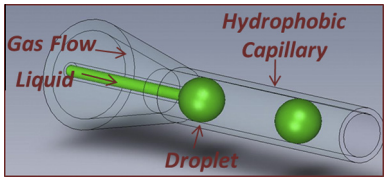

ARTICLE INFO

Article history:
Received 7 December 2014
Accepted 8 February 2015
Available online 13 February 2015

Keywords:
Microfluidics
Droplets
Dripping mode

ABSTRACT

Microfluidic schemes for forming uniform aqueous microdroplets usually rely on contacting the aqueous liquid (dispersed phase) with an immiscible oil (continuous phase). Here, we demonstrate that the oil can be substituted with gas (nitrogen or air) while still retaining the ability to generate discrete and uniform aqueous droplets. Our device is a capillary co-flow system, with the inner flow of water getting periodically dispersed into droplets by the external flow of gas. The droplet size and different formation modes can be tuned by varying the liquid and gas flow rates. Importantly, we identify the range of conditions that correspond to the "dripping mode", i.e., where discrete droplets are consistently generated with no satellites. We believe this is a significant development that will be beneficial for chemical and biological applications requiring clean and contaminant-free droplets, including DNA amplification, drug encapsulation, and microfluidic cell culture.

1. Introduction

Conventional droplet microfluidics involves the formation of discrete microscale droplets within microchannels [1,2]. Droplets generated by microfluidics tend to be very uniform in size, and their high surface-to-volume ratios allow for rapid diffusion and heat transfer with their surroundings [3]. Accordingly, such droplets have been explored as microreactors or assay containers [4,5], templates for particle synthesis [6], cell carriers [7,8], and even computing logic units [9]. Droplets are usually formed by contacting two immiscible liquid streams within the device: e.g., a stream of water (dispersed phase, DP) and a stream of oil (continuous phase, CP). At the meeting point of the streams (e.g., at a T-junction), the CP induces shear forces that pinch off the DP into individual droplets. The resulting aqueous droplets are transported within the oily CP, with surfactants in the CP stabilizing the interface and thus preventing coalescence of adjacent droplets [2,3].

Thus far, the use of a liquid as *both* continuous and dispersed phases is considered foundational in the field of droplet microfluidics. However, several limitations arise due to the use of immiscible liquids. For example, in the case where aqueous droplets are crosslinked into microparticles or microgels, the particles still need to be washed to remove residual oil from their surfaces. Often,

* Corresponding authors at: Department of Chemical and Biomolecular Engineering, University of Maryland, College Park, MD 20742, United States (S.R. Raghavam).
E-mail addresses: ddev@umd.edu (D.L. DeVoe), sraghava@umd.edu (S.R. Raghavan).

http://dx.doi.org/10.1016/j.jcis.2015.02.023
0021-9797/

multiple washing steps are required, and these steps almost always have to be conducted off-chip. This is especially problematic if the particles are employed to encapsulate biological payloads such as cells or proteins – the washing steps can then negatively impact the viability of the encapsulants. In other cases, the water/oil interface constrains the utility of the on-chip droplets. For example, during DNA amplification within droplets via the polymerase chain reaction (PCR), it is known that the key enzyme involved in polymerizing DNA (Taq polymerase) irreversibly binds and denatures at the water/oil interface, thus reducing the efficiency of amplification [5]. Moreover, surfactants that are added to the continuous phase for droplet stabilization can act as a source of contamination, with adverse effects for biological and chemical assays [3].

In this paper, we investigate an alternative to conventional droplet microfluidics, in which gas (nitrogen or air) is used to replace oil as the CP fluid. In this water-in-gas (W/G) approach, aqueous droplets are generated within a gaseous continuous phase, thereby ensuring that the droplets are inherently free of oil and surfactant contamination. Our focus is on establishing a microfluidic W/G platform that offers robust and repeatable operation, stable generation of individual droplets at periodic intervals, and precise control of droplet size. Toward this end, we have constructed a device based on concentric glass capillaries with their inner surfaces rendered hydrophobic. Water (DP) is sent through the inner capillary while gas (CP) flows through the outer surrounding capillary. At the meeting point of the streams, uniform water droplets are produced, with the size and periodicity of the droplets controlled by the water and gas flow rates. The droplets remain intact while traveling downstream, allowing them to be further manipulated or collected for analysis. We find that discrete droplets with no satellites are produced for a set of flow rates, and we map out the different droplet formation regimes.

To our knowledge, W/G droplet generation within microfluidic devices has not yet been studied systematically, and is not currently used by most researchers. This is possibly due to a lack of systematic guidelines for producing uniform droplets in W/G setups. It should be noted, though, that the dispersion of liquid streams into droplets using air has been widely studied for applications in ink-jet printers, sprayers and atomizers [10–12]. However, the droplets in those cases are dispersed into open environments, not in microchannels. Also, processes like atomization produce a wide distribution of droplet sizes rather than a uniform population. More recently, a few studies have been published on contacting water and gas streams within enclosed microfluidic devices [13,14] and inside the flow channels of polymer electrolyte membrane fuel cells [15,16]. While these studies have clarified the underlying physics, their focus was not on forming uniform droplets. Here, we work with a microfluidic setup and flow conditions (relatively low gas velocities, i.e., below 3 m/s) that are different from previous studies. Our main interest is in establishing guidelines for the generation of uniform aqueous droplets of a given size.

2. Results and discussion

The microfluidic device used for W/G droplet formation consists of a capillary co-flow generator connected to a long downstream flow pathway, as shown in Fig. 1A. The device is fabricated by inserting an inner capillary into a larger outer capillary to form a simple co-flow device (both capillaries are made out of fused quartz) [17,18]. The dispersed liquid phase (W) is introduced through the inner capillary while the continuous gas phase (G) flows through the outer capillary. Both phases flow in the same direction, and the two meet at the tip of the inner capillary, producing aqueous droplets (Fig. 1B).

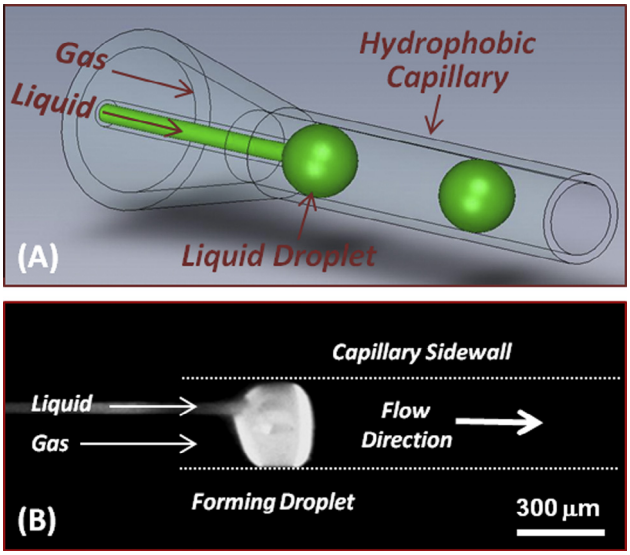

Fig. 1. Microfluidic device used in this study for generating liquid droplets using gas as the continuous phase. The device is configured with an inner glass capillary (50 μm ID, 80 μm OD) inserted co-directionally into an outer glass capillary (300 μm ID). The inner surfaces of both capillaries are rendered hydrophobic. Liquid (water) is introduced through the inner capillary as the dispersed phase (DP) while gas (nitrogen) through the outer capillary phase serves as the continuous phase (CP). At the tip of the inner capillary, uniform liquid droplets are formed periodically and these are broken off and carried away by the gas flow. (A) is a schematic of the device while (B) is a photograph of the device in operation. The photograph shows the liquid droplet right before it breaks off from the capillary tip. Dotted lines in the photograph indicate the sidewall boundaries of the outer capillary.

The wetting behavior of the channel wall is critically important for stable W/G droplet generation. In conventional W/O or O/W droplet generation, the surface chemistry of the channel walls is engineered to promote wetting of the continuous phase, with a hydrophobic surface for W/O droplets or a hydrophilic surface for O/W droplets. Thereby, contact between the dispersed phase and the channel walls is minimized or eliminated. However, in the case of W/G droplet generation, the low density of the gas phase cannot prevent direct contact between the aqueous droplets and the channel wall. Hence, it is critical for the channel wall to be highly non-wetting to the dispersed (W) phase. We therefore treated the capillaries with octadecyltrimethoxysilane, an 18-carbon long silane that anchors to the silanols on the surface of the glass (quartz) capillary while presenting a dense layer of hydrophobic alkyl groups to the aqueous droplets. It should also be noted that, due to the lack of a lubrication layer, imperfections in the channel walls can exert drag on the droplets, disturbing and potentially breaking them into smaller satellite droplets. In that context, our quartz capillaries are relatively smooth and present minimal surface roughness and imperfections.

Droplet formation is initiated by injecting the dispersed phase (W) through the inner capillary, with the flow rate controlled by a syringe pump. We added sodium fluorescein (0.1 wt%) to the water to allow visual monitoring of the droplets by a fluorescence microscope. The continuous phase (G) is delivered from a tank of compressed nitrogen (or air) with pressure controlled by a regulator. An in-line mass flow sensor is used to measure the gas flow rate during experiments. Typical flow rates of the liquid (W) phase are around 500 nL/min whereas the flow rates of the gas (G) are about 10,000 times higher, i.e., around 5×10^6 nL/min.

It is worth discussing the constraints on gas flow rates in the present system. In conventional W/O or O/W microfluidic droplet generation, the W and O fluids meet at a junction where droplets

are produced through a balance between viscous stresses acting on the emerging droplet and interfacial tension [3,19,20]. Due to high liquid viscosities, the viscous stresses are relatively high even at low flow rates of the CP, and so the forces necessary for droplet formation are readily achieved. However, in the case of W/G droplet generation, the low viscosity of the gas (CP) results in lower viscous stresses on the emerging liquid droplet under identical flow conditions. To achieve stresses that are sufficiently large to induce the formation of discrete liquid droplets, the gas flow rate must be increased without exceeding a value beyond which atomization of the droplet occurs [10]. This sets the range for the gas flow rates used here.

Our experiments show that near-monodisperse populations of aqueous droplets are formed over a range of liquid and gas flow rates (SI Movie 1). The droplets in this case have consistent volumes and well-defined periodicity. Fig. 2A shows a series of images revealing the droplet formation process in this case, which we term the "dripping mode" due to its similarity to a mode of the same name in conventional W/O or O/W droplet formation [3]. As the liquid emerges out of the tip of the inner capillary, it develops a characteristic near-spherical profile due to the surface tension of water (Image A0). Thereafter, as the liquid at the capillary tip increases in volume, the gap between the liquid surface and channel walls reduces, leading to a rapid increase in viscous stress on the liquid (Images A1, A2). When the viscous stress exceeds the interfacial tension holding the liquid to the tip of the inner capillary, the droplet is pinched off and emitted from the tip before being carried downstream by the gas (Image A3). Under certain flow conditions, the droplet can fill the entire channel prior to pinch-off, as shown previously in Fig. 1B. In this case, a thin gap supporting gas flow past the liquid volume must remain until the droplet is released from the inner capillary.

We have identified two primary droplet formation modes over the range of flow rates explored here. The first is the dripping mode described in Fig. 2A and SI Movie 1, which leads to uniform droplets. A second is the "satellite-forming mode" where large polydisperse primary droplets are generated alongside smaller satellite droplets (Fig. 2B and SI Movie 2). In the latter mode, which occurs at high liquid and low gas flow rates, each emerging aqueous droplet is broken into multiple smaller droplets. The image sequence in Fig. 2B shows that the initial part of this mode is similar to that of the dripping mode, with a near-spherical volume of liquid emerging from the inner capillary tip (Image B0). However, after growing to a certain size, the primary droplet splits into smaller satellite droplets (Images B1, B2). Because the majority of the satellite droplets are much smaller than the outer capillary diameter, the gas cannot exert sufficient momentum to carry these droplets downstream and they can become attached to the sidewall before evaporating or merging into a subsequent primary droplet.

Phase diagrams displaying the flow conditions leading to each mode of droplet formation are presented in Fig. 3. These data correspond to liquid flow rates from 200 to 800 nL/min, while the gas flow rates were between 3.2×10^6 and 12.8×10^6 nL/min. The

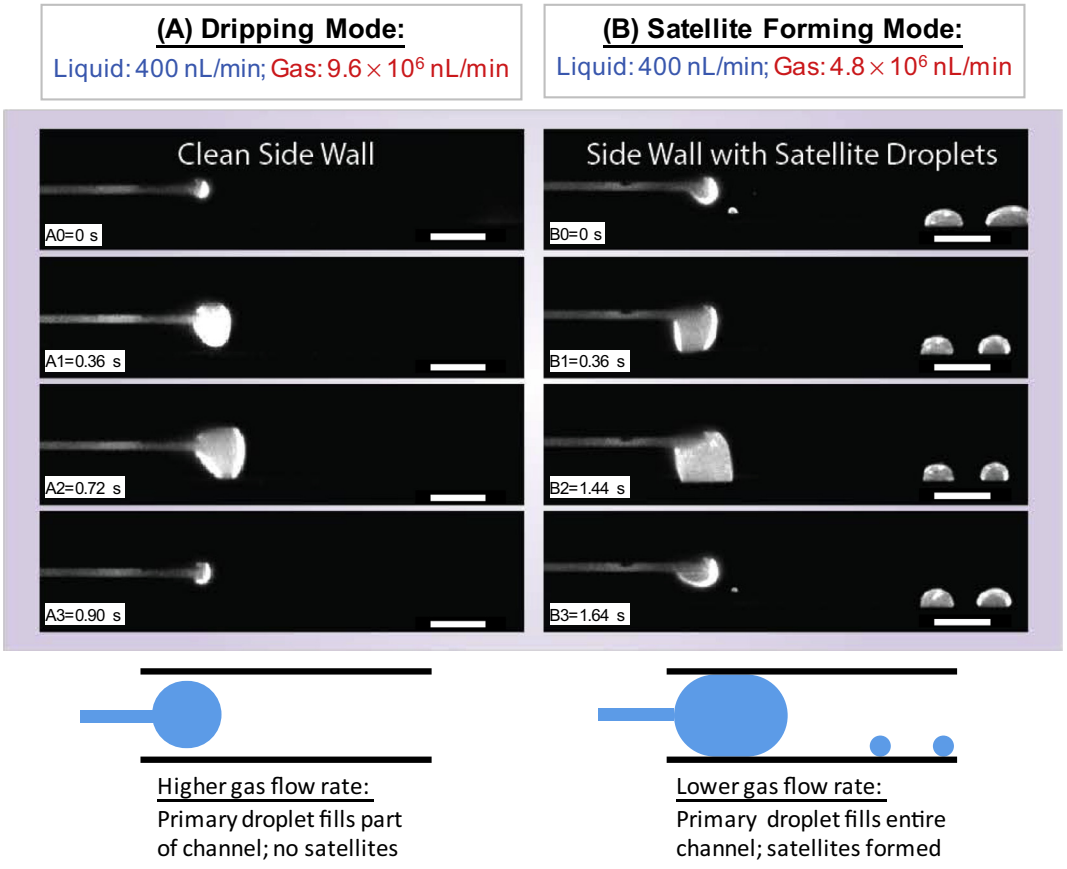

Fig. 2. Time-lapse photographs depicting the two different W/G droplet formation modes. (A) *Dripping Mode*: In this mode, discrete, uniform droplets of water are formed periodically (see SI Movie 1). The water droplet grows at the tip of the inner capillary (A0–A2) before it is pinched off (A3) and carried away by the flow of gas. Note that the sidewall of the outer capillary remains clean in this case, i.e., no droplets remain attached to it. (B) *Satellite-Forming Mode*: This mode occurs at lower gas flow rates than in the dripping mode. In this case, the droplet formed at the capillary tip is not stable and portions of the growing droplet (B0–B2) break up into smaller satellites (see SI Movie 2). Note also that the satellite droplets tend to get stuck on the capillary sidewall. Scale bars are 300 μm in all images. Schematics of the two modes are shown below the photographs.

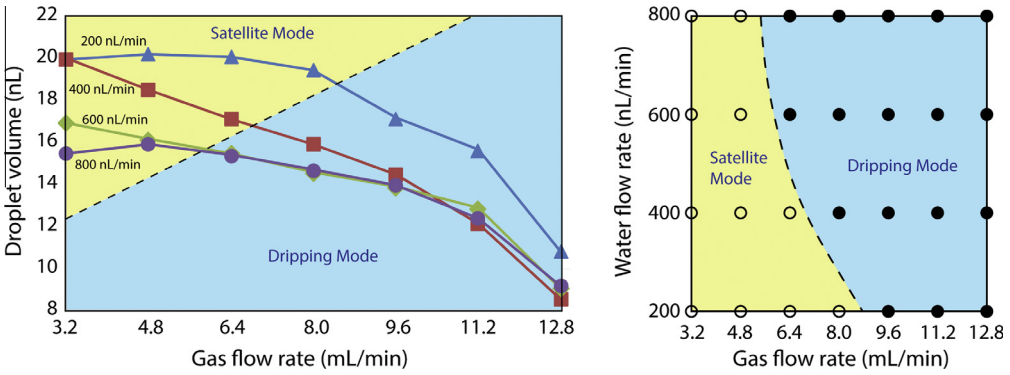

Fig. 3. Phase diagrams showing the W/G droplet formation modes under different gas and liquid flow rates. (Left) Plot of the primary droplet volume vs. the gas (CP) flow rate for different values of the liquid (DP) flow rate. (Right) Plot of the liquid (DP) vs. gas (CP) flow rates. In both figures, the dashed line demarcates the transition from the dripping mode to the satellite-forming mode. Note that the dripping mode occurs at higher gas flow rates.

estimates of primary droplet volume are obtained from the known aqueous flow rates and measurements of the primary droplet frequency. A key finding from Fig. 3 is that, for a given liquid flow rate, increasing the gas flow rate causes a transition from the satellite-forming mode to the dripping mode. The transition is reversed by decreasing the gas flow rate, with no observed hysteresis (SI Movie 3). The satellite-forming mode thus occurs at lower gas flow rates, with a strong dependence on the gas:liquid flow rate ratio. This observation contrasts with liquid-in-liquid droplet formation, where satellite droplets occur only in a "jetting mode" at high flow rates of the continuous phase due to droplet destabilization from excessive viscous forces [2]. While similar jetting mode behavior has been observed in liquid–gas droplet generators at high gas flow rates (this is akin to atomization) [14], the formation of satellite droplets at low gas flow rates has not been previously reported to our knowledge.

Over the range of flow rates explored in this work, the dripping mode is the dominant regime, supporting the stable formation of monodisperse aqueous droplets with average diameters in the range between 250 and 320 μm. As seen in Fig. 3, droplet size within the dripping mode is relatively insensitive to liquid flow rate, particularly at higher values of this parameter. This behavior is different from W/O or O/W droplet generators, where droplet size is largely a function of flow rate ratio [21,22]. Note that as the gas flow rate is lowered, the primary droplet increases in volume and increasingly fills up the volume of the channel.

The transition between dripping and satellite-forming modes occurs in the limit when the primary droplet fills up the entire channel, i.e., when the primary droplet diameter d is (slightly) larger than the channel diameter D = 300 μm. (Note that a spherical droplet of 300 μm diameter has a volume of 13.7 nL. For higher d, the droplet at the capillary tip is elongated into a plug before pinch-off; see schematic in Fig. 2). As the droplet size approaches this limit, the gas flow path is nearly completely occluded, but there remains a small gap h between the droplet boundary and the channel walls. At this stage, the hydrodynamic inertial and pressure forces acting on the drop become very high since these forces $\sim(D/h)^2$ [13,14]. In other words, the smaller the gap h between the channel and the droplet, the larger these forces, which counteract the surface tension forces that keep the droplet attached to the tip of the inner capillary. Overall, this is an unstable scenario and it results in the formation of satellites in addition to the primary droplets. Our observations suggest that there is an upper limit to the size of uniform droplets that can be produced in the dripping mode using the W/G approach. To a first approximation, this upper limit is simply dictated by the channel dimensions and it can be varied by altering the diameter of the outer capillary.

Droplets formed under both the dripping and satellite modes were collected off-line by immersing the outlet of the outer capillary into an external glass vial filled with hexadecane mixed with 2 wt% of the nonionic surfactant Span 80. The aqueous droplets remain stabilized against coalescence in the vial. Droplets formed in the dripping mode are highly uniform in size, forming a hexagonal-close-packed array when observed under an optical microscope (Fig. 4A). These droplets have an average diameter of 262 μm, with a standard derivation of only 3 μm (Fig. 4, right panel). The uniformity of these droplets not only demonstrates

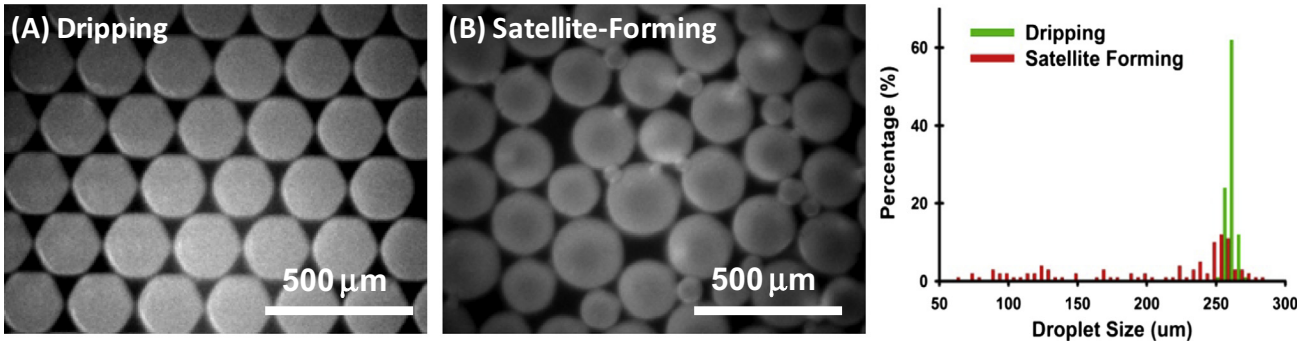

Fig. 4. Microscopic images and size distributions of aqueous droplets generated in the dripping and satellite-forming mode. At the capillary outlet, droplets stained with a fluorescent dye are collected in a vial filled with oil and surfactant. The resulting droplets are imaged by optical microscopy and images of droplets are shown for (A) dripping mode (liquid flow rate 800 nL/min, gas flow rate 12×10^6 nL/min) and (B) satellite-forming mode (liquid flow rate 400 nL/min, gas flow rate 4×10^6 nL/min). In the panel on the right, the size distributions of droplets in (A) and (B) are plotted as histograms, with the data corresponding to a sample size of 100 droplets in each case.

the controlled nature of the dripping mode, but also reveals that droplets remain intact and discrete as they travel down the channel to the capillary exit. This latter point is consistent with optical observation of the entire process (SI Movie 4). On the other hand, droplets within the satellite-forming regime are polydisperse (Fig. 4B) and widely distributed in size (Fig. 4, right panel).

3. Conclusions

We have demonstrated the continuous production of uniform aqueous droplets in a surrounding gas (nitrogen or air) stream within a microfluidic capillary co-flow device. Controlling the wetting properties of the capillaries is crucial for successful droplet formation. Droplet formation follows two modes: dripping and satellite-forming. We have constructed phase diagrams from experimental data identifying the flow rates associated with each mode. The transition from dripping to satellite-forming mode occurs when the gas flow rate is lowered, and it seems to correlate with the occlusion of the entire channel by the growing liquid droplet. Thus, this transition depends on the flow rates as well as the dimensions of the channel (outer capillary). Our work provides guidance for further investigations of liquid-in-gas droplet formation. Potential future directions include *in situ* droplet polymerization into solid or gel-like microparticles, and the use of droplets as microreactors and containers for biological assays. In all these cases, the utility of our approach lies in the ability to generate droplets that are free from oil and surfactant contamination. This approach could also be used to generate uniform droplets of other liquids, including polar ones like alcohols or nonpolar ones like hydrocarbons. The key will be to tailor the surface properties of the channel walls such that it is non-wetting to the liquid at hand.

4. Materials and methods

Octadecyltrimethoxysilane, sorbitan-monooleate (Span 80), hexadecane and sodium fluorescein were obtained from Sigma–Aldrich. All chemicals were used as received. Fused quartz capillaries of different diameters (50 μm ID/80 μm OD and 300 μm ID/400 μm OD) were purchased from VitroCom. All capillaries were modified to be hydrophobic by immersion into a 0.1 M HCl solution for 30 min at 70 °C, rinsing with DI water, and drying before being put into an vacuum oven together with an open volume (3 mL) of octadecyltrimethoxysilane at 60 °C overnight.

The microfluidic co-flow capillary devices were assembled from the hydropholically modified glass capillaries in a manner similar to previous designs [17,18]. The inner glass capillary (50 μm ID) was first connected to one end of a 2.5 cm length of 250 μm ID and 750 μm OD Tygon tubing (Cole-Parmer). The other end of the Tygon tubing was inserted into a 10 μL plastic pipette tip with the end cut off. The open capillary end was positioned within the modified pipette top with a ~2 cm length outside the tip head. After inserting another Tygon tubing segment into the tail of the pipette for convenient introduction of the gas continuous phase, the tail was sealed with epoxy. At the pipette tip, the other end of the inner glass capillary was inserted into the 300 μm ID outer sheath capillary, and the tip of the pipette was sealed with epoxy. The overall length of the inner channel over which droplets are formed was 10 cm.

The dispersed phase was DI water mixed with 0.1 wt% of sodium fluorescein, a water-soluble fluorescent dye. A precision syringe pump (Pump 11 Elite, Harvard Apparatus) was used to control the infusion of the dispersed phase into the device. For control of the gas flow, a compressed nitrogen tank was first connected to a low pressure regulator (Airgas 1–5 psi regulator) equipped with an in-line digital mass flow sensor (FMA3101, Omega Engineering) that monitored the real-time gas flow rate. Optical images and movies of droplet formation were taken using an inverted fluorescent microscope (Nikon Eclipse TE2000s). Droplet sizes during droplet formation were determined through the known flow rate of the dispersed phase and the measured droplet generation frequency. Droplets were also collected off-line in a glass vial filled with hexadecane mixed with 2 wt% of Span 80 surfactant. Sizes of these droplets were determined from optical microscope images using the Nikon NIS-Elements software.

Acknowledgments

This work was partially funded by grants from the UMD Center for Energetic Concepts Development and from DARPA. AXL was supported by a SMART scholarship from the Department of Defense.

Appendix A. Supplementary material

Movies showing the two droplet generation modes, i.e., dripping (Movie 1) and satellite-forming (Movie 2), the transition between the two modes (Movie 3), and downstream droplet transport and collection (Movie 4).

Supplementary data associated with this article can be found, in the online version, at http://dx.doi.org/10.1016/j.jcis.2015.02.023.

References

[1] R.K. Shah, H.C. Shum, A.C. Rowat, D. Lee, J.J. Agresti, A.S. Utada, L.-Y. Chu, J.-W. Kim, A. Fernandez-Nieves, C.J. Martinez, D.A. Weitz, Mater. Today 11 (2008) 18–27.
[2] S.-Y. Teh, R. Lin, L.-H. Hung, A.P. Lee, Lab Chip 8 (2008) 198–220.
[3] R. Seemann, M. Brinkmann, T. Pfohl, S. Herminghaus, Rep. Progr. Phys. 75 (2012) 016601.
[4] H. Song, J.D. Tice, R.F. Ismagilov, Angew. Chem. Int. Ed. 42 (2003) 768–772.
[5] S.L. Angione, A. Chauhan, A. Tripathi, Anal. Chem. 84 (2012) 2654–2661.
[6] J.I. Park, A. Saffari, S. Kumar, A. Günther, E. Kumacheva, Annu. Rev. Mater. Sci. 40 (2010) 415–443.
[7] J.F. Edd, D. Di Carlo, K.J. Humphry, S. Koster, D. Irimia, D.A. Weitz, M. Toner, Lab Chip 8 (2008) 1262–1264.
[8] J. Clausell-Tormos, D. Lieber, J.-C. Baret, A. El-Harrak, O.J. Miller, L. Frenz, J. Blouwolff, K.J. Humphry, S. Köster, H. Duan, C. Holtze, D.A. Weitz, A.D. Griffiths, C.A. Merten, Chem. Biol. 15 (2008) 427–437.
[9] M. Prakash, N. Gershenfeld, Science 315 (2007) 832–835.
[10] A.M. Gañán-Calvo, Phys. Rev. Lett. 80 (1998) 285–288.
[11] L. Martín-Banderas, M. Flores-Mosquera, P. Riesco-Chueca, A. Rodríguez-Gil, Á. Cebolla, S. Chávez, A. Gañán-Calvo, Small 1 (2005) 688–692.
[12] R. Ledesma-Aguilar, R. Nistal, A. Hernández-Machado, I. Pagonabarraga, Nat. Mater. 10 (2011) 367–371.
[13] B. Carroll, C. Hidrovo, J. Fluid. Eng. 135 (2013) 071206.
[14] B.C. Carroll, Droplet Generation and Mixing in Confined Gaseous Microflows, Ph.D. Dissertation, University of Texas, 2012.
[15] C.E. Colosqui, M.J. Cheah, I.G. Kevrekidis, J.B. Benziger, J. Power Sources 196 (2011) 10057–10068.
[16] M.J. Cheah, I.G. Kevrekidis, J.B. Benziger, Langmuir 29 (2013) 9918–9934.
[17] C. Arya, J. Kralj, K. Jiang, M.S. Munson, T.P. Forbes, D. DeVoe, S.R. Raghavan, S.P. Forry, J. Mater. Chem. B 1 (2013) 4313–4319.
[18] K. Jiang, A. Sposito, J. Liu, S.R. Raghavan, D.L. DeVoe, Polymer 53 (2012) 5469–5475.
[19] D.R. Link, S.L. Anna, D.A. Weitz, H.A. Stone, Phys. Rev. Lett. 92 (2004) 054503.
[20] S.L. Anna, N. Bontoux, H.A. Stone, Appl. Phys. Lett. 82 (2003) 364–366.
[21] P. Garstecki, H.A. Stone, G.M. Whitesides, Phys. Rev. Lett. 94 (2005) 164501.
[22] Z. Nie, M. Seo, S. Xu, P. Lewis, M. Mok, E. Kumacheva, G. Whitesides, P. Garstecki, H. Stone, Microfluid. Nanofluid. 5 (2008) 585–594.